Available online at www.sciencedirect.com
ScienceDirect
JOURNAL OF ELECTRON SPECTROSCOPY and Related Phenomena
Journal of Electron Spectroscopy and Related Phenomena 156–158 (2007) 303–306
www.elsevier.com/locate/elspec

Effect of phase composition on X-ray absorption spectra of ZrO_2 thin films

A. Kikas [a,*], J. Aarik [a], V. Kisand [a], K. Kooser [a], T. Käämbre [a], H. Mändar [a], T. Uustare [a], R. Rammula [a,b], V. Sammelselg [b], I. Martinson [c]

[a] *Institute of Physics, University of Tartu, Riia 142, 51014 Tartu, Estonia*
[b] *Institute of Physical Chemistry, University of Tartu, Jakobi 2, 51014 Tartu, Estonia*
[c] *Department of Physics, Lund University, P.O. Box 118, SE-22100 Lund, Sweden*

Available online 28 November 2006

Abstract

The X-ray photoabsorption spectra of ZrO_2 films with different phase compositions were measured. The analysis of the results obtained shows that due to the site-sensitivity the X-ray photoabsorption spectroscopy is an attractive method for characterization of the ZrO_2 structure. This allows application of the X-ray spectroscopy in investigation of the crystal structure in the various stages of the thin film growth including the initial stage of the ZrO_2 growth.
© 2006 Elsevier B.V. All rights reserved.

Keywords: Zirconium dioxide; X-ray absorption spectra; Atomic layer deposition

1. Introduction

Zirconium dioxide (ZrO_2) is a material that has been extensively studied in last few years. The main interest in this material has been due to its perspective applications in integrated circuits, magnetic random access memories and read heads. In the integrated circuits, ZrO_2 can be used as a high-permittivity (high-*k*) gate dielectric of field-effect transistors [1–4]. In the magnetic random access memories and read heads, ZrO_2 can be used as a barrier layer in spin-dependent tunnel junctions [5]. A specific feature of these applications is that ultrathin films of few nanometers in thickness are needed in the devices [1–5]. When developing methods for processing this kind of films, characterization techniques with high spatial resolution are usually needed. Therefore, electron spectroscopy methods are frequently employed to obtain information on the composition and character of chemical bonds of ZrO_2 thin films [2,4,6,7]. In addition, the band-gap energy of ZrO_2 has been estimated from the XPS data [8,9].

Our earlier study of various titanium dioxide phases [10] has shown that X-ray absorption spectra (XAS) are sensitive to the thin film structure. For this reason we also performed similar investigation for ZrO_2 thin films, which most frequently crystallize in monoclinic [7,11–15], tetragonal [7,11–16] and/or cubic [12,15,17] phases. The films studied in this work were grown by the atomic layer deposition (ALD) method. This deposition technique was chosen because it had allowed most precise control of the thin film growth and had widely been used for processing high-*k* dielectrics [2,3,7–9,11–15] that can be applied in microelectronic devices of the next generations. In addition, monoclinic, tetragonal, cubic and amorphous phases can reproducibly be obtained and stabilized in ALD films when using appropriate process parameters [11–15].

2. Experimental

The films were grown in a flow-type ALD reactor on single crystal silicon substrates using $ZrCl_4$ and H_2O as the precursors. In more detail, the deposition procedure has been described in an earlier paper [15]. In order to obtain thin films with different phase compositions, we varied the film thickness, *d*, and growth temperature, T_G (Table 1). The film thicknesses were calculated from electron probe microanalysis (EPMA) and X-ray fluorescence (XRF) data [18,19] using films grown on fused silica substrates as reference samples. The thickness values of the latter films were determined from the spectral oscillations of the optical transmission spectra.

* Corresponding author. Tel.: +372 7374617; fax: +372 7383033.
E-mail address: Arvo.Kikas@ut.ee (A. Kikas).

0368-2048/$ – see front matter © 2006 Elsevier B.V. All rights reserved.
doi:10.1016/j.elspec.2006.11.031

For characterization of the phase composition, we applied the reflection high-energy electron diffraction (RHEED) and X-ray diffraction (XRD) methods. The former method yielded information from a surface layer with the thickness of few nanometers whereas the latter one characterized the overall phase compositions of the films. Lattice parameters determined for the dominating crystalline phases were $a_c = 509 \pm 1$ pm for the cubic phase, $a_t = 357 \pm 2$ pm and $c_t = 518 \pm 2$ pm for the tetragonal phase and $a_m = 511 \pm 3$ pm, $b_m = 521 \pm 2$ pm, $c_m = 535 \pm 2$ pm and $\beta_m = 99.2°$ for the monoclinic phase. The space groups were $P4_2/nmc$ in the case of tetragonal phase and $P12_1/c1$ in the case of monoclinic phase.

The elemental composition of the films investigated in this work was studied earlier [15,19,20]. According to these studies the O/Zr ratio was 2.0 ± 0.1 independently of the deposition process parameters. In the films grown at 500–600 °C, the concentration of residual chlorine and hydrogen impurities did not exceed the detection limit, which was 0.1–0.2 at.%. The concentration of the impurities increased, however, with decreasing deposition temperature. The concentrations were 1.5 at.% for H and 0.8 at.% for Cl in the films grown at 300 °C and as high as 6 at.% for H and 4.7 at.% for Cl in the films grown at 180 °C [19,20].

The XAS were measured at beamline D1011 of MAX-II storage ring (Lund, Sweden) as a total electron yield using the microchannel plate detector. For excitation the SX-700 monochromator with 16 μm slit size was used, which provides the energy resolution about 200 meV at the O 1s photoabsorption edge and 100 meV at Zr 3p photoabsorption edge. The reference signal from the gold mesh was used for the normalization of the spectra. The energy scales of different spectra were aligned using the chromium absorption structure in the raw spectra. As the XAS were measured as the total yield of emitted electrons, there dominate the slow secondary electrons with escape depth about 10 nm. Thus, our XAS characterize the surface layer with the thickness of some tens of nanometers.

3. Results and discussion

XRD and RHEED studies (Table 1) demonstrated that at the low deposition temperatures (180 °C) the initial stage of growth gave an amorphous film (sample A1), but prolonged growth yielded a film, which was a mixture of the amorphous and cubic phases (sample C1). We verified that heat treatment of amorphous films at 400 °C during a time period, which was comparable to the growth duration of the thickest films, caused no crystallization. Thus, at 180 °C, the crystallization of the cubic phase evidently started only on the surface of growing film when sufficient thickness was reached. Nevertheless, as indicate the RHEED data the crystallization was not complete even at the surface of films that were as thick as 250 nm.

In case of the samples M1 and M2 the bulk sensitive XRD method showed the presence of monoclinic and tetragonal phases, whereas the surface-sensitive RHEED was able to detect only the monoclinic phase. Therefore the growth of tetragonal phase, dominating at 300–600 °C in the case of thinner films (samples T1–T3), was replaced with the growth of monoclinic phase when a certain film thickness was obtained. More detailed RHEED studies revealed that the growth of the monoclinic phase started to dominate when the film thickness exceeded 250–300 nm at 300 °C, 50–100 nm at 500 °C and 40–50 nm at 600 °C. According to XRD data, the relative amount of the monoclinic phase was about 90 mass% in the 230 nm thick film grown at 500 °C. Consequently, no additional tetragonal phase was formed at higher deposition temperatures when the crystallization of monoclinic phase became possible. Moreover, it is possible that the tetragonal phase, which had been deposited in the beginning of growth process, partially transformed into the monoclinic phase in thicker films. In any case, the samples M1 and M2 contained mainly the monoclinic phase in their outermost layers with the thicknesses of at least 130 and 110 nm, respectively.

The Zr 3p edge XAS of the films (Fig. 1(a)) shows two strong multicomponent bands, with energetic separation of approximately 13 eV, which is in good agreement with the spin–orbit splitting of Zr 3p level (13.7 eV). These spectra are very similar to the absorption spectra measured earlier for zirconium silicate alloys, prepared by the plasma enhanced chemical vapor deposition [21]. According to Ref. [21] the features in photoabsorption can be assigned to the transitions from the Zr 3p level to the conduction band states with Zr 4d origin (double bands at 332–334 and 346–348 eV) and Zr 5s origin (shoulder at 344 eV and band at 358 eV). Basically the absorption spectra of different polymorphs are similar, only in the spectra for tetragonal samples the intensities for first subpeaks at 332 and 334 eV are reversed, which indicates, that the changes in the local structure in photoabsorption site are reflected in XAS spectrum. Also the shoulder corresponding to the transitions to states with Zr 5s ori-

Table 1
Phase compositions of ZrO_2 thin films

Sample number	T_G (°C)	Number of cycles	Thickness (nm)	Phase composition	
				RHEED	XRD
A1	180	300	50	Amorphous	Amorphous
C1	180	1500	250	Amorphous + cubic	Amorphous + cubic
T1	300	500	70	Tetragonal	Tetragonal
T2	500	500	50	Tetragonal	Tetragonal
T3	600	300	30	Tetragonal	Tetragonal
M1	500	2000	230	Monoclinic	Monoclinic + tetragonal
M2	600	1500	160	Monoclinic	Monoclinic + tetragonal

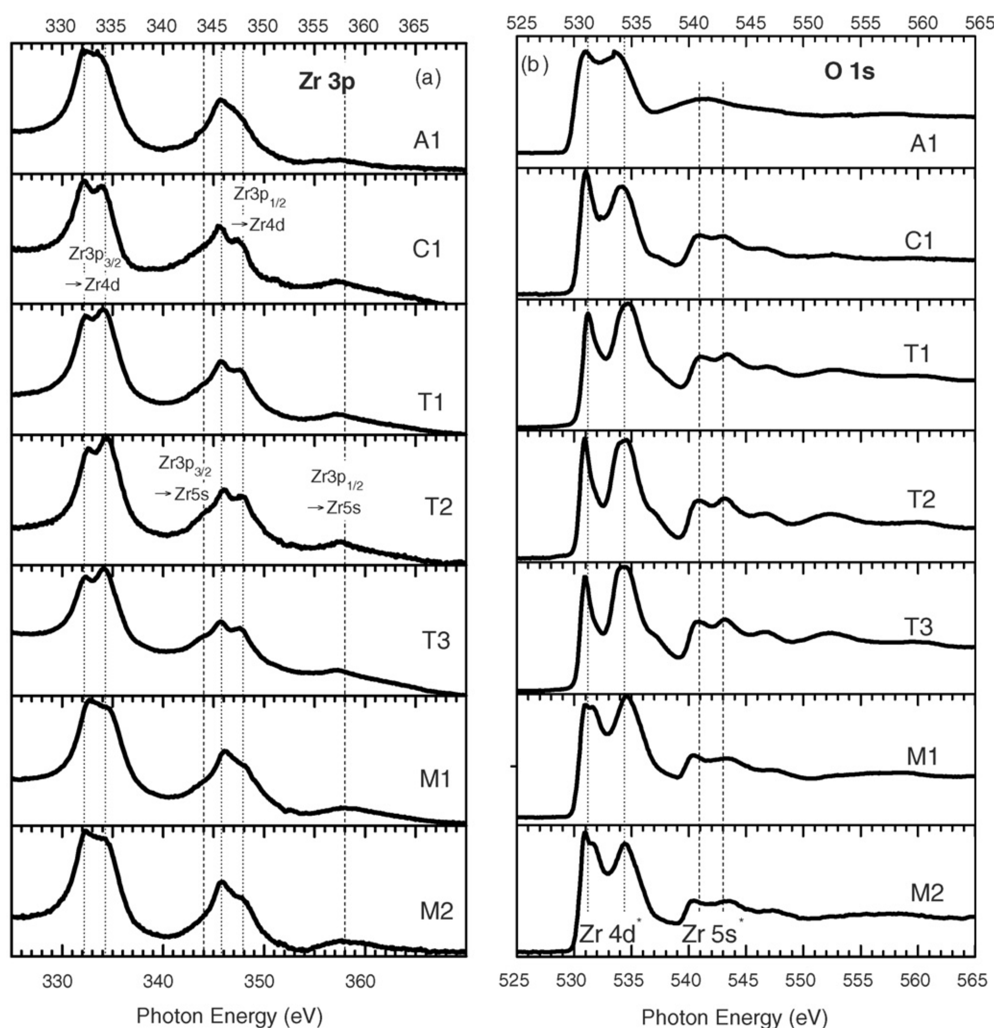

Fig. 1. Zr 3p (panel (a)) and O 1s (panel (b)) X-ray absorption spectra of ZrO_2 films with various phase compositions (see Table 1). Film A1 has amorphous structure, C1 cubic, T1–T3 tetragonal and M1–M2 monoclinic structure. The spectra are normalized to the same maximum intensity after the subtraction of constant background.

gin at 344 eV is better resolved in spectra of tetragonal samples. Note, that in the spectra of amorphous sample (A1) these elements of structure are not well resolved, probably due to different local environments for absorption-site atoms.

The shapes of the O 1s edge photoabsorption spectra (Fig. 1(b)) more significantly depend on the phase composition. Main elements in the spectra are maxima at 531, 534, 540 and 543 eV. These spectra can be divided into two energy regions. According to Refs. [21,22], at the energies 530–537 eV dominate the transitions from O 1s states to O 2p final states, which are hybridized with the Zr 4d states, split by the crystal field effects. The two peaks in this region, 531 and 534 eV can be attributed to the corresponding 4d states of e_g and t_{2g} symmetry, correspondingly [22]. Similarly to Zr 3p XAS, in the spectra of amorphous sample (A1) these elements of structure are not well resolved. In the spectra of the cubic and tetragonal samples, the first peak at 531 eV is well resolved and for tetragonal sample the second maximum at 534 eV seems to consist of two overlapping maxima. In case of monoclinic samples (M1 and M2) the peak at 531 eV is splitted into two subpeaks (with energy separation about 1 eV). According to the XRD data (Table 1) these samples contain also the tetragonal phase and this may be a reason for the appearance of the first subpeak, which energetically overlaps with peak in spectra of tetragonal phase. RHEED patterns do not show, however, the tetragonal phase at the outermost surface of those films. Thus, the contribution of the tetragonal phase cannot be significant.

Above 538 eV the structures are due to oxygen 2p states mixed with Zr 5s states, which are pushed up in energy due to the larger oxygen 2p–metal 5sp interactions. According to Ref. [22], the intensity ratio of the d- and s-bands is directly related to relative hybridization strength. For this reason we can conclude, that there are no strong changes in hybridization effects for different polymorphs.

Comparing the XAS spectra of the tetragonal samples T1–T3 with each other, one can see no significant differences, although the growth temperatures, thicknesses and impurity concentrations of these films differed markedly. A similar conclusion can be drawn comparing the spectra of the monoclinic samples M1 and M2. Consequently, the variation in the growth temperature of

a certain crystalline phase, related changes in the concentration of impurities and defects, and contribution of the surface effects were not able to cause changes comparable to those resulted by the phase transitions.

4. Conclusions

This study demonstrates that the XAS spectra are sensitive to the amorphous–cubic and tetragonal–monoclinic phase transitions in ZrO_2. Although the sensitivity to the cubic–tetragonal transition is lower, some conclusions about this transition can be made too. As our experiments showed, even significant variation of the processing parameters and concentration of impurities in the films did not cause any changes in the XAS spectra that would be comparable to those caused by the phase transitions. Therefore, the photoabsorption spectroscopy can be used for detection of different ZrO_2 phases. Due to the sensitivity to symmetry at absorption site of the photoabsorption process, the XAS spectra can also be applied to characterize the phase transitions that often take place during the thin film growth. However, it should be kept in mind that in case of mixtures of different crystal structures characteristic features in XAS may overlap and this possibility should be taken into account in analysis. Also the additional theoretical calculations of XAS for different crystal structures of ZrO_2 will facilitate the detailed analysis.

Acknowledgements

The authors wish to thank staff of MAX-lab for the support during measurements. The Financial support by the Estonian Science Foundation (grant nos. 5861, 6536, and 6651), Nordforsk, Physiographic Society in Lund, Carl Trygger Foundation, and the European Community—Research Infrastructure Action under the FP6 "Structuring the European Research Area" Programme (through the Integrated Infrastructure Initiative "Integrating Activity on Synchrotron and Free Electron Laser Science") is gratefully acknowledged.

References

[1] T. Ngai, W.J. Qi, R. Sharma, J.L. Fretwell, X. Chen, J.C. Lee, S.K. Banerjee, Appl. Phys. Lett. 78 (2001) 3085.
[2] C.M. Perkins, B.B. Triplett, P.C. McIntyre, K.C. Saraswat, S. Haukka, M. Tuominen, Appl. Phys. Lett. 78 (2001) 2357.
[3] H.S. Chang, S. Jeon, H. Hwang, D.W. Moon, Appl. Phys. Lett. 80 (2002) 3385.
[4] R. Mahapatra, J.-H. Lee, S. Maikap, G.S. Kar, A. Dhar, N.-M. Hwang, D.-Y. Kim, B.K. Mathur, S.K. Ray, Appl. Phys. Lett. 82 (2003) 4331.
[5] J. Wang, P.P. Freitas, E. Snoeck, P. Wei, J.C. Soares, Appl. Phys. Lett. 79 (2001) 4387.
[6] G. Lucovsky, J. Non-Cryst. Solids 303 (2002) 40.
[7] S.K. Dey, C.-G. Wang, D. Tang, M.C. Kim, R.W. Carpenter, C. Werkhoven, E. Shero, J. Appl. Phys. 93 (2003) 4144.
[8] H. Nohira, W. Tsai, W. Besling, E. Young, J. Petry, T. Conard, W. Vandervorst, S. De Gendt, M. Heyns, J. Maes, M. Tuominen, J. Non-Cryst. Solids 303 (2002) 83.
[9] R. Puthenkovilakam, J.P. Chang, Appl. Phys. Lett. 84 (2004) 1353.
[10] R. Ruus, A. Kikas, A. Saar, A. Ausmees, E. Nõmmiste, J. Aarik, A. Aidla, T. Uustare, I. Martinson, Solid State Commun. 104 (1997) 199.
[11] C. Zhao, G. Roebben, H. Bender, E. Young, S. Haukka, M. Houssa, M. Naili, S. De Gendt, M. Heyns, O. Van Der Biest, Microelectron. Reliab. 41 (2001) 995.
[12] K. Kukli, K. Forsgren, J. Aarik, T. Uustare, A. Aidla, A. Niskanen, M. Ritala, M. Leskelä, A. Hårsta, J. Cryst. Growth 231 (2001) 262.
[13] S. Ferrari, D.T. Dikadjevi, S. Spiga, G. Tallarida, C. Wiemer, M. Fanciulli, J. Non-Cryst. Solids 303 (2002) 29.
[14] M. Cassir, F. Goubin, C. Bernay, P. Vernoux, D. Lincot, Appl. Surf. Sci. 193 (2002) 120.
[15] J. Aarik, A. Aidla, H. Mändar, T. Uustare, V. Sammelselg, Thin Solid Films 408 (2002) 97.
[16] C.R. Aita, E.E. Hoppe, R.S. Sorbello, Appl. Phys. Lett. 82 (2003) 677.
[17] A. Mehner, H. Klümper-Westkamp, H. Hoffmann, P. Mayr, Thin Solid Films 308/309 (1997) 363.
[18] V. Sammelselg, J. Aarik, A. Aidla, A. Kasikov, E. Heikinheimo, M. Peussa, L. Niinistö, J. Anal. Atom. Spectrom. 14 (1999) 523.
[19] V. Sammelselg, E. Rauhala, K. Arstila, A. Zakharov, J. Aarik, A. Kikas, J. Karlis, A. Tarre, A. Seppälä, J. Asari, I. Martinson, Mikrochim. Acta 139 (2002) 165.
[20] K. Kukli, M. Ritala, J. Aarik, T. Uustare, M. Leskelä, J. Appl. Phys. 92 (2002) 1833.
[21] G. Lucovsky, G.B. Rayner Jr., Y. Zhang, C.C. Fulton, R.J. Nemaish, G. Appel, H. Ade, J.L. Whitten, Appl. Surf. Sci. 212/213 (2003) 563.
[22] L. Soriano, M. Abbate, J.C. Fuggle, M.A. Jimenez, J.M. Sanz, C. Mythen, H.A. Padmore, Solid State Commun. 87 (1993) 699.